nature immunology

c-Myc-induced transcription factor AP4 is required for host protection mediated by CD8+ T cells

Chun Chou[1], Amelia K Pinto[2], Jonathan D Curtis[1], Stephen P Persaud[1], Marina Cella[1], Chih-Chung Lin[1], Brian T Edelson[1], Paul M Allen[1], Marco Colonna[1], Erika L Pearce[1], Michael S Diamond[1–3] & Takeshi Egawa[1]

Although the transcription factor c-Myc is essential for the establishment of a metabolically active and proliferative state in T cells after priming, its expression is transient. It remains unknown how T cell activation is maintained after c-Myc expression is downregulated. Here we identified AP4 as the transcription factor that was induced by c-Myc and sustained activation of antigen-specific CD8+ T cells. Despite normal priming, AP4-deficient CD8+ T cells failed to continue transcription of a broad range of c-Myc-dependent targets. Mice lacking AP4 specifically in CD8+ T cells showed enhanced susceptibility to infection with West Nile virus. Genome-wide analysis suggested that many activation-induced genes encoding molecules involved in metabolism were shared targets of c-Myc and AP4. Thus, AP4 maintains c-Myc-initiated cellular activation programs in CD8+ T cells to control microbial infection.

Protective immunity by CD8+ T cells is critical for host defense against many pathogens that cause death or chronic infection. During acute infection by a virus or intracellular bacterium, antigen-specific CD8+ T cells are primed by signaling via the T cell antigen receptor (TCR), costimulatory molecules and cytokine receptors and undergo rapid population expansion, effector differentiation and memory cell formation[1,2]. In the priming phase, an activated CD8+ T cells becomes larger by increasing global gene transcription and protein translation and uses aerobic glycolysis pathways to produce the energy and materials needed for biosynthesis before entry into the cell cycle[3–7]. Published studies have established that the transcription factor c-Myc is essential for the initiation of the global cellular activation processes in activated lymphocytes as well as in cancer and embryonic stem cells[8–11]. Expression of c-Myc is induced by signaling through the TCR and the receptor for interleukin 2 (IL-2R)[12], and c-Myc is essential for the metabolic reprogramming and growth of T cells[13].

During acute infection, the population expansion of CD8+ T cells persists even after levels of antigen and inflammation wane[4]. While this persistent proliferation may be driven by residual antigen on antigen-presenting cells, other evidence suggests that optimally primed CD8+ T cells continue to proliferate after antigen and cytokines decrease to suboptimal concentrations[14–17]. The expression of c-Myc is rapidly induced in activated T cells[9,13]. Its expression, however, does not persist throughout the duration of T cell population expansion[9,18]. These findings suggest that other transcription factors maintain c-Myc-initiated cellular activation to maximize the clonal expansion and effector differentiation of T cells during acute responses to pathogen infection.

We hypothesized that signaling via the TCR and cytokine receptors during the early stage of pathogen infection induces transcription factors that program CD8+ T cells for a durable response. Among the cytokines established as being important for CD8+ T cell responses, IL-2 sustains clonal expansion *in vitro* and possibly *in vivo*[19–21] and promotes effector differentiation[20,22,23]. In this study, we identified AP4 as a transcription factor regulated by IL-2R signaling and demonstrated that AP4 sustained the proliferation of antigen-specific CD8+ T cells in a cell-autonomous way in models of acute infection. CD8+ T cells from mice lacking AP4 were able to initiate rapid clonal expansion similar to that of cells from age-matched wild-type mice but failed to sustain the rapid clonal expansion rates of wild-type cells, which led to a much lower clonal frequency at the peak of response. Control of infection with West Nile virus (WNV) in the central nervous system (CNS), which requires sustained antigen-specific CD8+ T cell responses for host-mediated clearance and survival, was compromised in mice lacking AP4 specifically in CD8+ T cells. Finally, our data suggested that AP4 sustained cellular activity through the regulation of a substantial proportion of genes that are targets of c-Myc. Thus, our data establish that AP4 regulates the magnitude of acute responses by CD8+ T cells to control microbial infection.

RESULTS

Regulation of AP4 by signaling via the TCR and IL-2R

By microarray analysis, we identified ~70 transcription factor–encoding genes whose expression changed more than 1.8-fold in CD8+ T cells following neutralization of IL-2 (**Fig. 1a**). In addition to known IL-2-regulated genes such as *Bcl6* and *Eomes*[23], we identified *Tfap4* (which encodes AP4) as a gene dependent on signaling via IL-2R (**Fig. 1a**). AP4 is a basic helix-loop-helix protein that regulates the transcription of viral genes and repression of the gene encoding the

[1]Department of Pathology and Immunology, Washington University School of Medicine, Saint Louis, Missouri, USA. [2]Department of Medicine, Washington University School of Medicine, Saint Louis, Missouri, USA. [3]Department of Molecular Microbiology, Washington University School of Medicine, Saint Louis, Missouri, USA. Correspondence should be addressed to T.E. (tegawa@wustl.edu).

Received 9 October 2013; accepted 17 June 2014; published online 13 July 2014; doi:10.1038/ni.2943

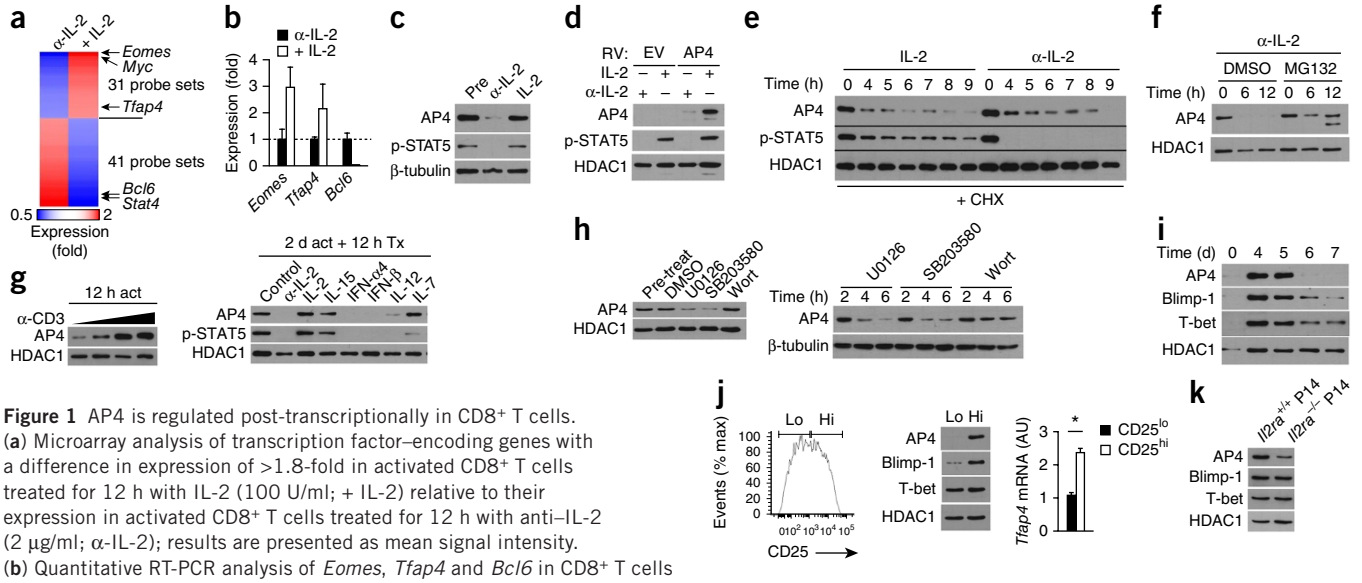

Figure 1 AP4 is regulated post-transcriptionally in CD8⁺ T cells. (**a**) Microarray analysis of transcription factor–encoding genes with a difference in expression of >1.8-fold in activated CD8⁺ T cells treated for 12 h with IL-2 (100 U/ml; + IL-2) relative to their expression in activated CD8⁺ T cells treated for 12 h with anti–IL-2 (2 μg/ml; α-IL-2); results are presented as mean signal intensity. (**b**) Quantitative RT-PCR analysis of *Eomes*, *Tfap4* and *Bcl6* in CD8⁺ T cells treated as in **a**; results for cells treated with IL-2 are presented relative to those of cells treated with anti–IL-2, set as 1 (dashed line). (**c**) Immunoblot analysis of AP4 in CD8⁺ T cells before treatment (Pre) or treated as in **a**; phosphorylated STAT5 (p-STAT5) and β-tubulin serve as loading controls. (**d**) Immunoblot analysis of AP4 in *Tfap4*$^{-/-}$ CD8⁺ T cells transduced with retrovirus (RV) containing an empty vector (EV) or vector expressing AP4 (above blot) and treated as in **a** (above lanes); the histone deacetylase HDAC1 serves as a loading control throughout. (**e**) Immunoblot analysis of AP4 in CD8⁺ T cells treated for 0–9 h (above lanes) with IL-2 or anti–IL-2 (above blot) in the presence of cycloheximide (10 μM). (**f**) Immunoblot analysis of AP4 in CD8⁺ T cells treated for 0–12 h (above lanes) with anti–IL-2 in the presence of dimethyl sulfoxide (DMSO) or the proteasome inhibitor MG132 (10 μM). (**g**) Immunoblot analysis of AP4 in CD8⁺ T cells stimulated for 12 h with increasing concentrations (wedge) of anti-CD3 (12 h act) or stimulated for 2 d with anti-CD3 alone (Control) or with subsequent treatment for 12 h with anti–IL-2 or various cytokines (above lanes; 2 d act + 12 h Tx). IFN, interferon. (**h**) Immunoblot analysis of AP4 in CD8⁺ T cells stimulated for 48 h with anti-CD3 and anti-CD28 alone (Pre-treat) or subsequently treated for 6 h with DMSO, U0126, SB203580 or wortmannin (Wort) (left blot), or treated for 24 h with IL-2 followed by treatment for various times (above lanes) with U0126, SB203580 or wortmannin (right blot). (**i**) Immunoblot analysis of AP4, Blimp-1 and T-bet in P14 T cells adoptively transferred into host mice, assessed at 0–7 d (above lanes) after infection of the host with LCMV-Arm. (**j**) CD25 expression in CD44⁺CD62L⁻ CD8⁺ T cells from C57BL/6 mice at day 4.5 after infection with LCMV-Arm (left), and immunoblot analysis of AP4, Blimp-1 and T-bet (middle) and quantitative RT-PCR analysis of *Tfap4* (right) in the CD25^{lo} and CD25^{hi} cells sorted at left. (**k**) Immunoblot analysis of AP4 in *Il2ra*$^{+/+}$ and *Il2ra*$^{-/-}$ P14 donor T cells adoptively transferred into host mice and assessed on day 4 after infection of the host with LCMV-Arm. *$P < 0.05$ (unpaired *t*-test). Data are from one experiment (**a**), are pooled from two experiments (**b**; error bars, s.d.) or are representative of three experiments (**d**–**h**,**j**,**k**; error bars (**j**), s.d.), four experiments (**c**) or two experiments (**i**).

monomorphic coreceptor CD4 (*Cd4*)[24–26]. Although expression of *Tfap4* mRNA was reduced modestly upon withdrawal of IL-2, expression of AP4 protein was substantially diminished (**Fig. 1b**,**c**), which suggested that sustained AP4 expression required IL-2R signaling at both the transcriptional level and post-transcriptional level. The expression of AP4 from a retrovirus also required the stimulation of cells via IL-2R (**Fig. 1d**), which suggested its expression was regulated predominantly at the post-transcriptional level. The half-life of AP4 protein was 2–3 h under permissive conditions (with the addition of IL-2) or nonpermissive conditions (neutralization of IL-2) (**Fig. 1e**), with its degradation mediated by the ubiquitin-proteasome pathway (**Fig. 1f**). AP4 expression was sustained by TCR stimuli or other γ-chain cytokines (IL-7 and IL-15) but not by IL-12 or type I interferons (**Fig. 1g**). These results suggested that a common pathway converging from signaling via the TCR and IL-2Rγ chain sustained the expression of AP4 protein. Consistent with that, inhibitors of the mitogen-activated protein kinases MEK and p38 (U0126 and SB203580, respectively) attenuated the accumulation of AP4 protein in the presence of stimulation via the TCR or IL-2R (**Fig. 1h**). To confirm the roles of the TCR and IL-2R in maintaining AP4 expression *in vivo*, we obtained naive CD8⁺ T cells from P14 mice[27], which express a transgene encoding a TCR of α-chain variable region 2 and β-chain variable region 8 ($V_\alpha 2^+V_\beta 8^+$ TCR) specific for the epitope of amino acids 33–41 of lymphocytic choriomeningitis virus (LCMV) glycoprotein (gp(33–41)), then adoptively transferred those cells into wild-type host mice and acutely infected the host mice with the Armstrong strain of LCMV (LCMV-Arm) and assessed AP4 in the P14 cells. We found that the adoptively transferred LCMV-gp-specific P14 T cells had high expression of AP4 protein on days 4 and 5 after infection; this expression decreased on days 6 and 7 as T cell population expansion slowed markedly (**Fig. 1i**). In activated CD8⁺ T cells on day 4.5 after infection with LCMV-Arm, we detected AP4 protein specifically in CD25^{hi} cells but not in CD25^{lo} cells, despite the similar abundance of *Tfap4* mRNA in both subpopulations (**Fig. 1j**). Furthermore, P14 T cells lacking the gene encoding IL-2Rα (*Il2ra*$^{-/-}$ cells) had lower expression of AP4 protein than did their *Il2ra*$^{+/+}$ counterparts at 4 d after infection with LCMV-Arm (**Fig. 1k**). We concluded that AP4 was regulated post-transcriptionally in CD8⁺ T cells via signaling through the TCR and IL-2R *in vitro* and *in vivo*.

CD8⁺ T cell population expansion requires AP4

To assess the functions of AP4 in immune responses, we infected AP4-deficient (*Tfap4*$^{-/-}$) and congenic wild-type C57BL/6 mice with LCMV-Arm and examined the population expansion and differentiation of CD8⁺ T cells. At the peak of the response, the abundance of total CD8⁺ T cells and KLRG1⁺ terminally differentiated CD8⁺ T cells[1] was ~70% lower and 90% lower, respectively, in *Tfap4*$^{-/-}$ mice than in wild-type mice (**Fig. 2a**,**c**). The abundance of T cells specific for gp(33–41) was also 80% lower in *Tfap4*$^{-/-}$ mice than in wild-type mice and, among those cells, the abundance of KLRG1⁺ effector cells was

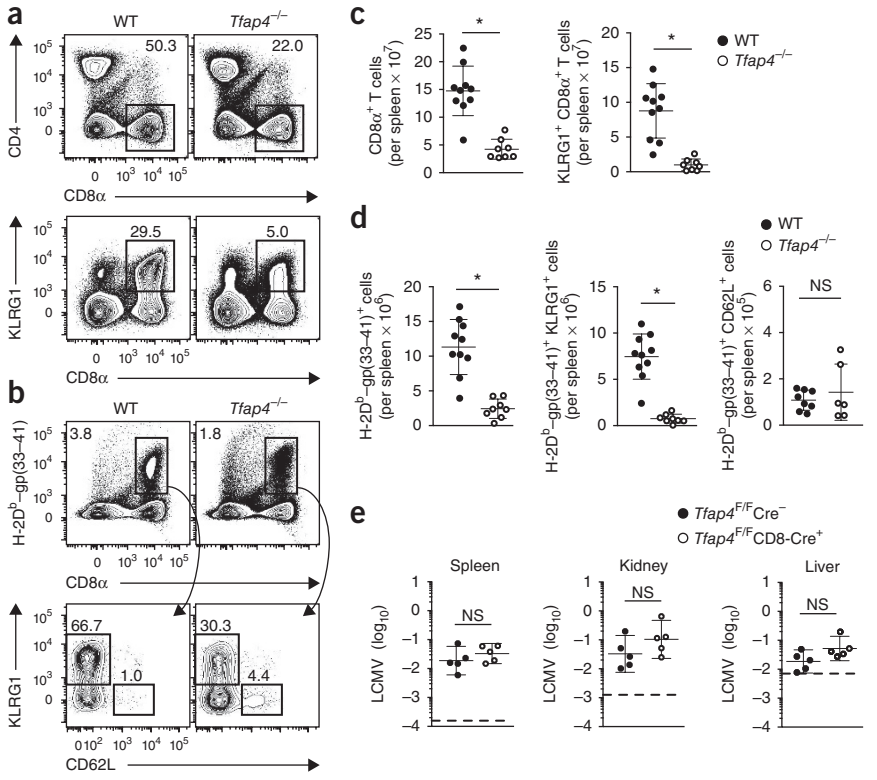

Figure 2 AP4 is required for the population expansion of antigen-specific CD8⁺ T cells following infection with LCMV-Arm. (**a**,**b**) Expression of CD4, CD8α and KLRG1 (**a**) and binding of an H-2D^b–gp(33–41) tetramer and expression of CD8α, KLRG1 and CD62L (**b**) in splenocytes from wild-type (WT) and *Tfap4*$^{-/-}$ mice, assessed by flow cytometry 8 d after infection with LCMV. Numbers adjacent to outlined areas (gates) indicate percent CD8α⁺ T cells (**a**, top), KLRG1⁺ CD8α⁺ effector cells (**a**, bottom), gp(33–41)-specific CD8α⁺ T cells among total splenocytes (**b**, top), and CD62L⁺ cells (top left) or KLRG1⁺ cells (bottom right) among gp(33–41)-specific CD8α⁺ T cells (**b**, bottom). (**c**,**d**) Cumulative results from **a** (**c**) and **b** (**d**): each symbol represents an individual mouse (n = 10 (wild-type) or 8 (*Tfap4*$^{-/-}$) mice); small horizontal lines indicate the mean (± s.d.). (**e**) Quantitative RT-PCR analysis of the abundance of transcripts encoding LCMV-gp in the spleen, kidneys and liver of *Tfap4*$^{F/F}$CD8-Cre⁺ and control *Tfap4*$^{F/F}$Cre⁻ mice 6 d after infection with LCMV-Arm; results are presented relative to those of control transcripts encoding hypoxanthine guanine phosphoribosyl transferase (*Hprt1*). Each symbol represents an individual mouse (n = 5 per genotype); small horizontal lines indicate the mean (± s.d.); long dashed horizontal lines indicate the limit of detection. NS, not significant; *P < 0.0001 (unpaired t-test). Data are representative of three experiments (**a**,**b**) or are pooled from three experiments (**c**,**d**) or two experiments (**e**).

diminished by 90% (**Fig. 2b**,**d**). To determine whether the requirement for AP4 was intrinsic to CD8⁺ T cells, we deleted a *lox*P-flanked *Tfap4* allele (*Tfap4*^{F}) specifically in CD8⁺ T cells with Cre recombinase transgenically expressed under the control of regulatory elements of the gene encoding CD8 that are active in post-selection thymocytes (CD8-Cre)[28] (**Supplementary Fig. 1a**,**b**). We observed a similar reduction in the number of total, KLRG1⁺ and gp(33–41)-specific CD8⁺ T cells in *Tfap4*$^{-/-}$ and *Tfap4*$^{F/F}$CD8-Cre⁺ mice relative to their abundance in wild-type mice (**Supplementary Fig. 1c**,**d**), which indicated that the requirement for AP4 was intrinsic to CD8⁺ T cells. The clonal expansion and effector differentiation of CD8⁺ T cells also were reduced in *Tfap4*$^{-/-}$ mice infected with *Listeria monocytogenes* expressing ovalbumin (LM-OVA) relative to that in wild-type mice (**Supplementary Fig. 2a**,**b**). Memory cells were generated and maintained similarly in *Tfap4*$^{-/-}$, *Tfap4*$^{F/F}$CD8-Cre⁺ and wild-type mice following infection with LCMV-Arm or LM-OVA (**Supplementary Fig. 3a–d**). However, the population expansion of *Tfap4*$^{-/-}$ and *Tfap4*$^{F/F}$CD8-Cre⁺ memory T cells was diminished relative to that of their wild-type counterparts upon secondary challenge (**Supplementary Fig. 3e–h**). Thus, AP4 was essential for the population expansion of antigen-specific CD8⁺ T cells both in primary responses and recall responses.

AP4 sustains CD8⁺ T cell clonal expansion

To compare the population expansion of *Tfap4*$^{-/-}$ and wild-type CD8⁺ T cells in an identical environment, we generated *Tfap4*$^{-/-}$ mice of the P14 mouse strain[27]. We mixed $V_\alpha2^+V_\beta8^+$ naive CD8⁺ T cells from *Tfap4*$^{-/-}$ (Thy-1.2⁺CD45.2⁺) P14 mice and *Tfap4*$^{+/+}$ (Thy-1.1⁺CD45.2⁺) P14 mice at a ratio of 1:1 and adoptively transferred the mixture into congenic wild-type (CD45.1⁺) host mice. Prior to infection with LCMV-Arm, the ratio of *Tfap4*$^{-/-}$ P14 T cells to *Tfap4*$^{+/+}$ P14 T cells remained approximately 1:1 in the spleen (**Fig. 3a**). That result was consistent with the similar frequency of CD8⁺ T cells in various tissues of *Tfap4*$^{-/-}$ and wild-type mice under steady-state conditions (**Fig. 3b**). To determine whether AP4 was required for the initial proliferation of P14 T cells, we labeled *Tfap4*$^{-/-}$ and *Tfap4*$^{+/+}$ P14 donor T cells with the division-tracking dye CFSE, then adoptively transferred the cells into wild-type (CD45.1⁺) host mice and infected the host mice with LCMV-Arm. On day 3 after infection, both *Tfap4*$^{-/-}$ P14 T cells and *Tfap4*$^{+/+}$ P14 T cells diluted CFSE to an undetectable level (**Fig. 3c**), consistent with the similar number of P14 T cells in the spleen and the frequency of cells positive for the thymidine analog BrdU following pulse labeling (**Fig. 3d–g**). These results established that AP4 was dispensable for the initial proliferation of CD8⁺ T cells during the antigen-specific response. Despite their rapid early population expansion, the absolute number of *Tfap4*$^{-/-}$ P14 donor cells was much lower than that of *Tfap4*$^{+/+}$ P14 donor cells at the peak of the response (**Fig. 3d–f**). Although *Tfap4*$^{-/-}$ P14 cells continued to proliferate until day 7 after infection, they failed to maintain rapid proliferation rates, as judged by BrdU pulse labeling on day 4 and later (**Fig. 3g**). Because CD8⁺ T cells divide six to seven times per day during a response to acute infection[29], the effect of a mild but continued decrease in the rate of incorporation of BrdU could theoretically result in a reduction in the clonal expansion of *Tfap4*$^{-/-}$ donor cells of over 90% compared with that of *Tfap4*$^{+/+}$ P14 donor cells over 4 d (**Fig. 3e**,**g**). We also observed reduced clonal expansion, incorporation of BrdU and activation of the metabolic checkpoint kinase mTOR pathway in *Tfap4*$^{-/-}$ OT-I T cells (which have transgenic expression of an ovalbumin-specific TCR) following infection with LM-OVA (**Supplementary Fig. 2c–e**). We did not, however, observe a difference between *Tfap4*$^{-/-}$ P14 T cells and *Tfap4*$^{+/+}$ P14 T cells in the frequency of annexin V–binding cells in those populations on day 6 (**Fig. 3h**,**i**) or in the ratio of *Tfap4*$^{-/-}$ P14 T cells to *Tfap4*$^{+/+}$ P14 T cells in various compartments on day

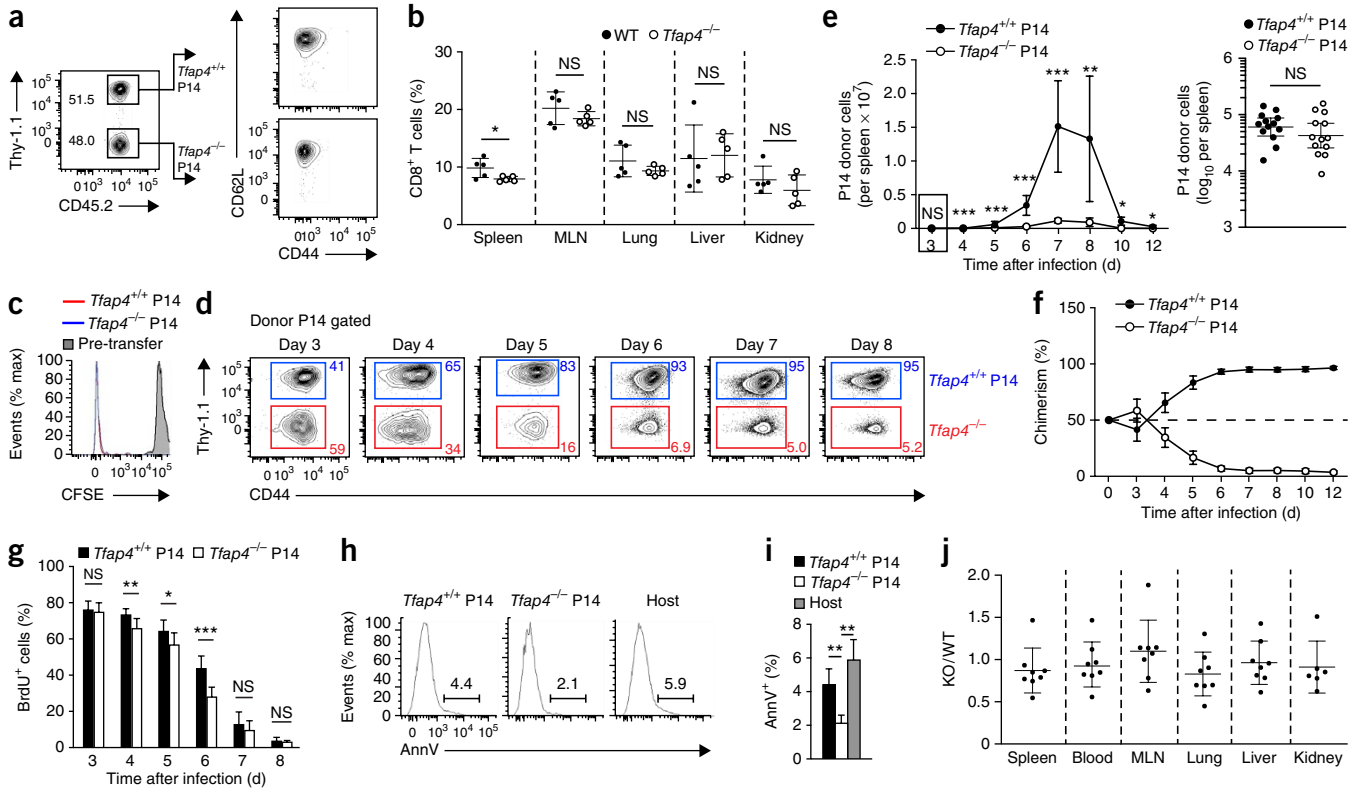

Figure 3 AP4 is required for the sustained clonal expansion of CD8$^+$ T cells but not for their initial proliferation. (**a**) Expression of CD62L and CD44 (right) by *Tfap4*$^{+/+}$ and *Tfap4*$^{-/-}$ P14 T cells (sorted by marker expression at left), assessed by flow cytometry 16 h after transfer together (at a ratio of 1:1) into congenic host mice. Numbers adjacent to outlined areas (left) indicate percent Thy-1.1$^+$CD45.2$^+$ (*Tfap4*$^{+/+}$) P14 T cells (top) or Thy-1.1$^-$CD45.2$^+$ (*Tfap4*$^{-/-}$) P14 T cells (bottom). (**b**) Frequency of CD8$^+$ T cells in the spleen, mesenteric lymph nodes (MLN), lungs, liver and kidneys of *Tfap4*$^{-/-}$ mice and control wild-type C57BL/6 mice (WT) under steady-state conditions. Each symbol represents an individual mouse; small horizontal lines indicate the mean (± s.d.). (**c**) Flow cytometry of CFSE-labeled *Tfap4*$^{+/+}$ and *Tfap4*$^{-/-}$ P14 donor T cells before transfer (Pre-transfer) and after transfer into host mice, assessed 3 d after infection of the host with LCMV-Arm. (**d**) Flow cytometry of *Tfap4*$^{+/+}$ and *Tfap4*$^{-/-}$ P14 donor cells transferred into host mice at a starting ratio of 1:1, assessed at various time points after infection of the host with LCMV-Arm (numbers in plots as in **a**). (**e**) Quantification of *Tfap4*$^{+/+}$ and *Tfap4*$^{-/-}$ P14 donor cells in the spleen of host mice as in **d** (n = 9–13 (day 3), 8–18 (day 4), 8–13 (day 5), 9–19 (day 6), 4–8 (day 7), 4–9 (day 8), 3 (day 10) or 5 (day 12)), normalized to 1 × 10^4 transferred cells (left), and data for day 3 (outlined at left) on a $\log_{10}$ scale (right): each symbol represents an individual mouse; small horizontal lines indicate the mean (± s.d.). (**f**,**g**) Frequency of *Tfap4*$^{+/+}$ and *Tfap4*$^{-/-}$ donor T cells in the mice in **e**, assessing chimerism (**f**), and frequency of BrdU$^+$ cells following 2 h of pulse labeling *in vivo* in those mice (**g**). (**h**) Binding of annexin V (AnnV) in *Tfap4*$^{+/+}$ and *Tfap4*$^{-/-}$ P14 donor cells and CD8$^+$CD44$^+$ effector host cells (Host) in the spleen 6 d after infection of the host with LCMV-Arm, assessed by flow cytometry. Numbers above bracketed lines indicate percent annexin V–positive cells. (**i**) Cumulative results from **h** (n = 5 host mice). (**j**) Ratio of *Tfap4*$^{-/-}$ P14 donor cells to *Tfap4*$^{+/+}$ P14 donor cells (KO/WT) (transferred at a starting ratio of 6:1) in various organs and blood of host mice 7 d after infection with LCMV-Arm. Each symbol represents an individual host mouse (n = 8); small horizontal lines indicate the mean (± s.d.). $^*P < 0.05$, $^{**}P < 0.01$ and $^{***}P < 0.001$ (unpaired t-test (**b**,**e**,**g**) or one-way analysis of variance (ANOVA) (**j**)). Data are representative of three (**a**,**d**) or two (**c**,**h**) experiments or are pooled from three (**b**,**e**–**g**) or two (**i**,**j**) experiments (error bars (**e**–**g**,**i**), s.d.).

7 after infection of the host with LCMV-Arm (**Fig. 3j**). These results suggested no substantial difference in the apoptosis or trafficking of antigen-specific T cells *in vivo*. Furthermore, it was unlikely that AP4 regulated the sensitivity of the TCR itself, since *Tfap4*$^{-/-}$ and *Tfap4*$^{+/+}$ OT-I T cells proliferated at similar rates and produced interferon-γ at similar frequencies in response to stimulation with the OVA peptide–pulsed irradiated wild-type splenocytes *in vitro* (**Supplementary Fig. 2f–h**). However, *Tfap4*$^{-/-}$ cells were outcompeted (in number) by *Tfap4*$^{+/+}$ cells during coculture, and *Tfap4*$^{-/-}$ cells failed to blast when incubated for 4 d or longer with irradiated splenocytes pulsed with 0.1 nM OVA peptide (**Supplementary Fig. 2f–h**). These results suggested that AP4 was required for sustained proliferation of T cells after stimulation of the TCR.

Protection against infection with WNV requires AP4

We next assessed the contribution of AP4 to CD8$^+$ T cell–mediated protection against a lethal infection in a model of infection with WNV. WNV is a virulent zoonotic virus that causes fatal encephalitis in humans and mice[30,31]. CD8$^+$ T cells are required for the clearance of WNV in both the spleen and the CNS[32]. To determine whether AP4 was required for protection against infection with WNV in a CD8$^+$ T cell–dependent manner, we infected *Tfap4*$^{F/F}$CD8-Cre$^+$ mice and age-matched control *Tfap4*$^{F/F}$Cre$^-$ mice with WNV. While the majority of *Tfap4*$^{F/F}$Cre$^-$ mice survived the infection, all *Tfap4*$^{F/F}$CD8-Cre$^+$ mice died between days 8 and 13 (**Fig. 4a**), similar to the death of WNV-infected mice lacking CD8$^+$ T cells[32]. *Tfap4*$^{F/F}$CD8-Cre$^+$ mice sustained higher viral loads in the brain than those of age- and sex-matched *Tfap4*$^{F/F}$Cre$^-$ mice on day 9 after infection (**Fig. 4b**), which indicated that AP4 expression in CD8$^+$ T cells was essential for the control of WNV in the CNS. The population expansion of CD8$^+$ T cells specific for the WNV nonstructural protein NS4B was diminished in WNV-infected *Tfap4*$^{-/-}$ and *Tfap4*$^{F/F}$CD8-Cre$^+$ mice compared with that of WNV-infected age- and sex-matched wild-type mice in the spleen on day 7 after infection (**Supplementary Fig. 4**). However,

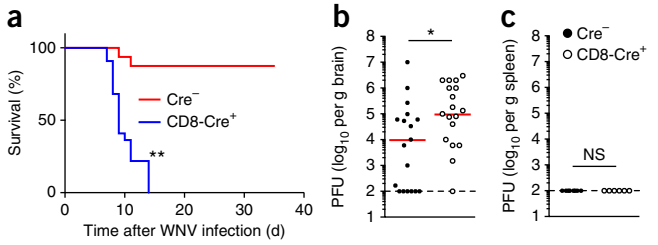

Figure 4 AP4 is essential for host protection against infection with WNV, in a CD8$^+$ T cell–intrinsic manner. (**a**) Survival of *Tfap4*$^{F/F}$Cre$^-$ control mice (Cre$^-$; $n = 16$) and *Tfap4*$^{F/F}$CD8-Cre$^+$ mice (CD8-Cre$^+$; $n = 22$) following infection with WNV. (**b**,**c**) Viral titers in the brain (**b**) and spleen (**c**) of *Tfap4*$^{F/F}$ Cre$^-$ and *Tfap4*$^{F/F}$ CD8-Cre$^+$ mice on day 9 after infection with WNV. Each symbol represents an individual mouse ($n = 18$ (**b**) or 7 (**c**) per genotype); red horizontal lines (**b**) indicate the median; dashed horizontal lines indicate limit of detection. $*P < 0.05$ and $**P < 0.001$ (log-rank test (**a**) or Mann-Whitney *U*-test (**b**,**c**)). Data are pooled from three (**a**), four (**b**) or two (**c**) independent experiments.

AP4 was dispensable for control of WNV in the spleen (**Fig. 4c**). Consistent with that observation, we detected no difference in burden of LCMV-Arm or LM-OVA in peripheral tissues following infection (**Fig. 2e** and **Supplementary Fig. 2i**), presumably because clearance of these pathogens begins at an early phase of the acute response. In contrast, AP4 was required for host protection against infection with WNV in the CNS (**Fig. 4a**,**b**), and AP4-mediated sustained activation of antigen-specific CD8$^+$ T cells may be critical for control of certain CNS pathogens.

AP4 sustains T cell activation

When T cells are primed, c-Myc activates aerobic glycolysis and amplifies global gene transcription and protein synthesis, which leads to cell growth and metabolic reprogramming[6,9,13,33]. The expression of c-Myc was induced rapidly after stimulation of the TCR, followed by upregulation of AP4 expression in CD8$^+$ T cells (**Supplementary Fig. 5a**,**b**). c-Myc was essential for the upregulation of AP4 expression in activated CD8$^+$ T cells, at the level of both protein and mRNA (**Fig. 5a**). In agreement with a published study[34], c-Myc bound to the *Tfap4* locus in activated CD8$^+$ T cells (**Supplementary Figs. 5c** and **6e**), which further suggested that AP4 expression was augmented by c-Myc through direct binding. In contrast to the defective growth and metabolic changes of *Myc*-deficient T cells[13], activated *Tfap4*$^{-/-}$ CD8$^+$ T cells underwent normal blast development accompanied by active glycolysis *in vitro* (**Supplementary Fig. 5d**–**f**). Moreover, *Tfap4*$^{-/-}$ and *Tfap4*$^{+/+}$ OT-I or P14 T cells were of similar size 3 d after infection with LCMV-Arm or LM-OVA (**Fig. 5b** and **Supplementary Fig. 5g**). The differences between *Tfap4*$^{-/-}$ and wild-type CD8$^+$ T cells in their gene expression either 3 d after activation *in vitro* or 2 d after infection with LM-OVA were substantially smaller than those observed at later time points, with alteration of few genes relevant to T cell activation (**Supplementary Fig. 5h**). Thus, AP4 was dispensable for establishment of the c-Myc-dependent cellular response to T cell activation. However, at later time points (days 4 and 6), *Tfap4*$^{-/-}$ OT-I or P14 T cells were smaller than their *Tfap4*$^{+/+}$ OT-I or P14 counterparts activated in the same host mice (**Fig. 5b**,**c** and **Supplementary Fig. 5g**). The difference between *Tfap4*$^{-/-}$ cells and control cells in terms of size coincided with the downregulation of c-Myc expression in antigen-specific CD8$^+$ T cells after infection with LM-OVA (**Fig. 5d**,**e**). A small fraction of OT-I T cells primed by infection of the host with LM-OVA upregulated c-Myc protein, as determined with a knock-in allele encoding a fusion of c-Myc and green fluorescent protein (c-Myc–GFP)[35]. Activated OT-I T cells uniformly expressed c-Myc–GFP as they increased in size until day 3 (**Fig. 5d**). Although the activated OT-I T cells continued to proliferate and only slowly reduced in size on day 4, their expression of c-Myc–GFP was downregulated by 95% compared with that on day 2 and by 90% compared with that on day 3 (**Fig. 5d**,**e**). In comparison, AP4 expression in wild-type cells also was upregulated following the induction of c-Myc and began to decrease on day 3 (**Fig. 5d**). In contrast to the rapid decay of c-Myc, we still detected AP4 protein on day 4 (**Fig. 5d**,**e**), which suggested that AP4 expression persisted longer than did c-Myc expression. Total RNA content per cell also was less in *Tfap4*$^{-/-}$ OT-I T cells than in *Tfap4*$^{+/+}$ OT-I T cells on day 4 (**Fig. 5f**). Furthermore, basal aerobic glycolysis and the maximum glycolytic capacity, as measured by the extracellular acidification rate (ECAR)[36], were significantly lower in *Tfap4*$^{-/-}$ OT-I cells than in *Tfap4*$^{+/+}$ OT-I cells recovered from the same host mice on days 4 and 6 after infection with LM-OVA (**Fig. 5g**). Consistent with that, expression of genes encoding key glycolytic enzymes (normalized to a per-cell basis through the use of 'spiked-in' control RNA[37]) was 30–60% lower and 75–80% lower in *Tfap4*$^{-/-}$ OT-I T cells than in *Tfap4*$^{+/+}$ OT-I T cells on days 4 and 6 after infection, respectively (**Fig. 5h**). These results indicated that AP4 was required for the sustained expression of genes encoding glycolytic molecules and suggested that AP4 sustained T cell activation after downregulation of c-Myc expression.

AP4 sustains c-Myc-initiated global cellular activity

To further define the requirement for AP4 in maintenance of the c-Myc-initiated T cell activation, we activated *Tfap4*$^{-/-}$ and *Tfap4*$^{+/+}$ OT-I T cells *in vivo* by adoptive transfer and infection of the host with LM-OVA and analyzed gene expression by microarray at the time point at which we had detected differences in cell size. For accurate assessment of gene expression, we 'spiked' the cellular RNA with a mixture of control RNAs according to the cell number and then profiled cell number–normalized gene expression in *Tfap4*$^{-/-}$ and *Tfap4*$^{+/+}$ OT-I T cells[9,10]. Consistent with the smaller size and lower RNA content of *Tfap4*$^{-/-}$ cells, global gene expression, as determined by the slopes of scatter plots, was lower in *Tfap4*$^{-/-}$ OT-I cells than in *Tfap4*$^{+/+}$ OT-I cells (**Fig. 6a**,**b**). We identified 1,784 genes with a difference in expression of more than 1.8-fold in *Tfap4*$^{-/-}$ OT-I cells versus *Tfap4*$^{+/+}$ OT-I cells at 4 d after infection with LM-OVA (**Fig. 6a**). Pathway analysis highlighted enrichment among the group of 1,784 genes for those encoding molecules related to metabolism, transcription and translation (**Fig. 6c**). To determine whether these genes were directly regulated by AP4, c-Myc or both, we performed chromatin immunoprecipitation (ChIP) analysis with antibody to AP4 (anti-AP4) and anti-c-Myc and profiled AP4- and c-Myc-bound genes in activated CD8$^+$ T cells (**Supplementary Fig. 6**). Unbiased analysis of 7,000 statistically significant peaks of binding of AP4 or c-Myc revealed that more than 50% of the AP4 and c-Myc peaks overlapped at the gene level (**Fig. 6d**). Furthermore, nearly a quarter (479 genes) of the 1,784 genes expressed differently in *Tfap4*$^{-/-}$ OT-I T cells versus *Tfap4*$^{+/+}$ OT-I T cells were bound by both AP4 and c-Myc (**Fig. 6d**). The group of shared targets of AP4 and c-Myc showed considerable enrichment for genes encoding molecules categorized as being involved in metabolism, transcription and translation pathways (**Fig. 6c** and **Supplementary Fig. 6e**). The majority of these 479 genes were upregulated in *Tfap4*$^{+/+}$ OT-I cells expressing both c-Myc and AP4 on day 2 after infection of the host with LM-OVA, continued to have high expression on day 4 when c-Myc levels waned, and were eventually downregulated on day 6 following the decrease in AP4 (**Fig. 6e**), which suggested that AP4 regulated these genes as c-Myc expression decayed. Because expression of these 479 genes was not different in *Tfap4*$^{-/-}$ OT-I T cells versus *Tfap4*$^{+/+}$

OT-I T cells on day 2 after infection (**Supplementary Fig. 5h**), the altered expression of these genes on day 4 might explain the phenotypes observed in *Tfap4*$^{-/-}$ OT-I T cells. Since we used cells coexpressing AP4 and c-Myc for the ChIP analysis, we further assessed whether AP4 still bound to these loci after downregulation of c-Myc expression by using CD25^{+} P14 T cells harvested from host mice 5 d after infection with LCMV-Arm. Although the expression of c-Myc was downregulated in P14 T cells on day 5 compared with its expression earlier time points (**Fig. 6f**), the majority of loci previously identified as being bound by both AP4 and c-Myc retained AP4 binding (**Fig. 6g**). These results suggested that c-Myc-induced AP4 expression was required for sustained transcription of c-Myc targets through direct binding.

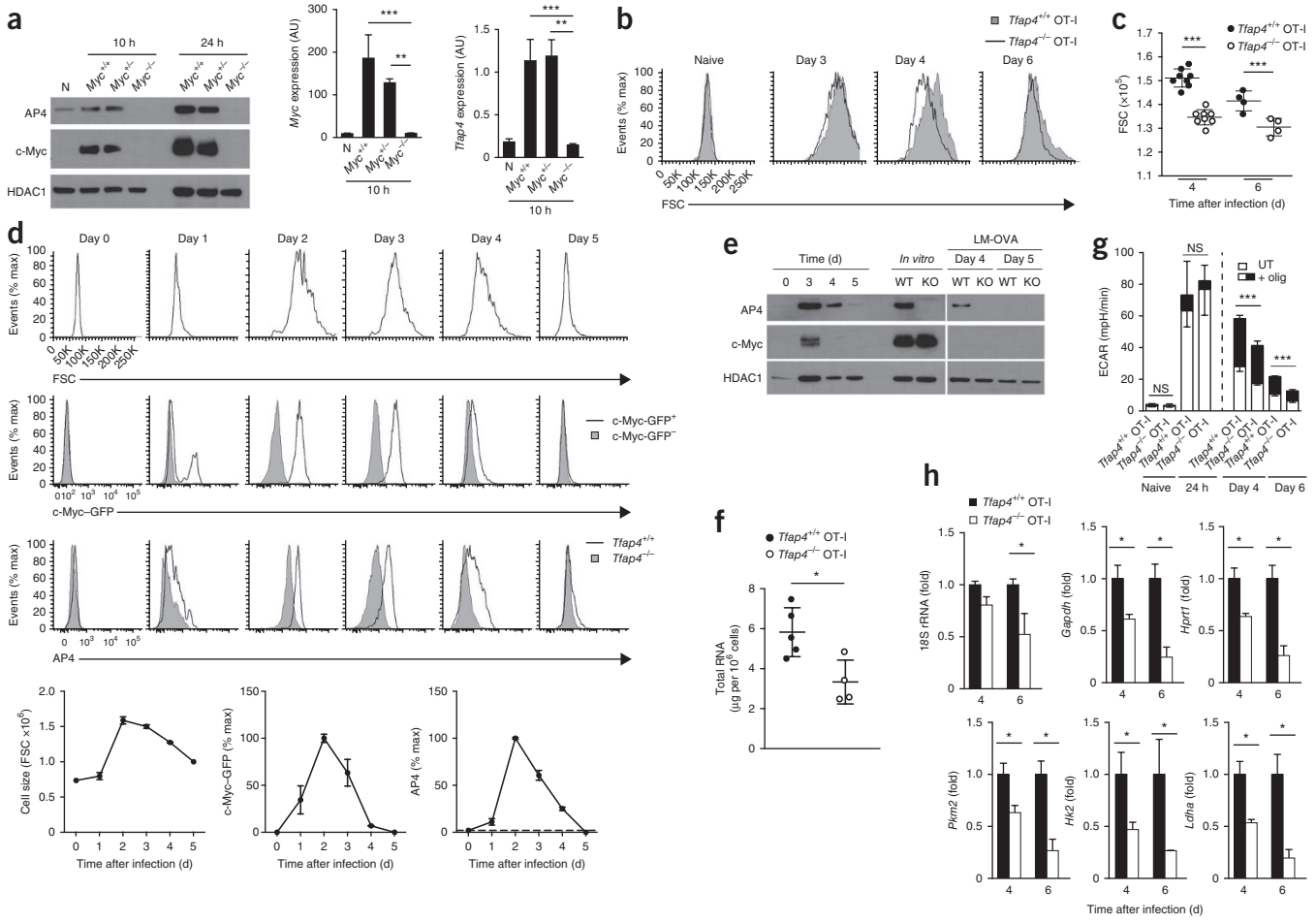

Figure 5 AP4 is induced by c-Myc and sustains glycolysis. (**a**) Immunoblot analysis of AP4 and c-Myc (top) and quantitative RT-PCR analysis of *Myc* and *Tfap4* (bottom) in wild-type naive CD8^{+} T cells treated with 4-hydroxytamoxifen (N) and in *Myc*$^{F/+}$Cre^{-} (*Myc*$^{+/+}$), *Myc*$^{F/+}$ *Rosa26*-Cre-ER^{T2} (*Myc*$^{+/-}$) and *Myc*$^{F/F}$ *Rosa26*-Cre-ER^{T2} (*Myc*$^{-/-}$) CD8^{+} T cells treated with 4-hydroxytamoxifen and stimulated for 10 or 24 h *in vitro* with anti-CD3 and anti-CD28. (**b**) Flow cytometry of *Tfap4*$^{+/+}$ and *Tfap4*$^{-/-}$ OT-I donor T cells adoptively transferred into host mice, assessed before (Naive) or 3, 4 or 6 d after infection of the host with LM-OVA, assessing cell size as forward scatter (FSC). (**c**) Cumulative results for cells as in **b**: each symbol represents an individual host mouse (n = 8 (day 4) or 4 (day 6)); small horizontal lines indicate the mean (± s.d.). (**d**) Size of *Tfap4*$^{+/+}$ OT-I donor T cells (assessed as forward scatter; top) and expression of c-Myc–GFP (middle) and AP4 (bottom) by *Tfap4*$^{+/+}$ and *Tfap4*$^{-/-}$ OT-I T cells on days 0–5 after infection with LM-OVA, assessed by flow cytometry; c-Myc–GFP results obtained by subtraction of autofluorescence from the GFP fluorescence of OT-I T cells heterozygous for the knock-in allele encoding c-Myc–GFP. Below, cumulative results obtained as above. (**e**) Immunoblot analysis of AP4 and c-Myc in *Tfap4*$^{+/+}$ OT-I donor T cells adoptively transferred into host mice, assessed in the naive state (0) or on days 3–5 after infection of the host with LM-OVA (left), and in *Tfap4*$^{+/+}$ (WT) and *Tfap4*$^{-/-}$ (KO) OT-I donor T cells activated for 24 h *in vitro* with anti-CD3 and anti-CD28 (*In vitro*) or adoptively transferred into host mice and activated *in vivo* by infection of the host for 4 or 5 d with LM-OVA (right), to demonstrate antibody specificity. (**f**) Total RNA in *Tfap4*$^{+/+}$ and *Tfap4*$^{-/-}$ OT-I donor T cells adoptively transferred into host mice and assessed 4 d after infection of the host with LM-OVA. Each symbol represents an individual host mouse (n = 5); small horizontal lines indicate the mean (± s.d.). (**g**) ECAR of *Tfap4*$^{+/+}$ and *Tfap4*$^{-/-}$ OT-I CD8^{+} T cells left unstimulated (Naive), stimulated for 24 h *in vitro* with anti-CD3 and anti-CD28 (middle) or adoptively transferred into host mice and analyzed on days 4 and 6 after infection of the host with LM-OVA, all assessed at baseline (without additional treatment (UT)) and after treatment with oligomycin (olig). (**h**) Quantitative RT-PCR analysis of genes encoding molecules involved in glycolysis in *Tfap4*$^{+/+}$ and *Tfap4*$^{-/-}$ OT-I T cells adoptively transferred into host mice and assessed on day 4 or 6 after infection of the host with LM-OVA; results were normalized to those of 'spiked-in' control RNA ERCC-00108 and are presented relative to those of *Tfap4*$^{+/+}$ OT-I T cells. $*P < 0.05$, $**P < 0.01$ and $***P < 0.001$ (one-way ANOVA (**a**), paired t-test (**c**) or unpaired t-test (**f**–**h**)). Data are representative of three experiments (**a**,**b** (day 4) and **d**,**e** (days 1–3)) or two experiments (**b** (day 6) and **d** (days 4–5)), are from one experiment (**d** (day 0)) or are pooled from three experiments (**a**,**c** (day 4) and **d**,**g** (days 1–3)) or two experiments (**c** (day 6) and **d**,**f**,**h** (days 4–5)); error bars (**a**,**d**,**g**,**h**), s.d.).

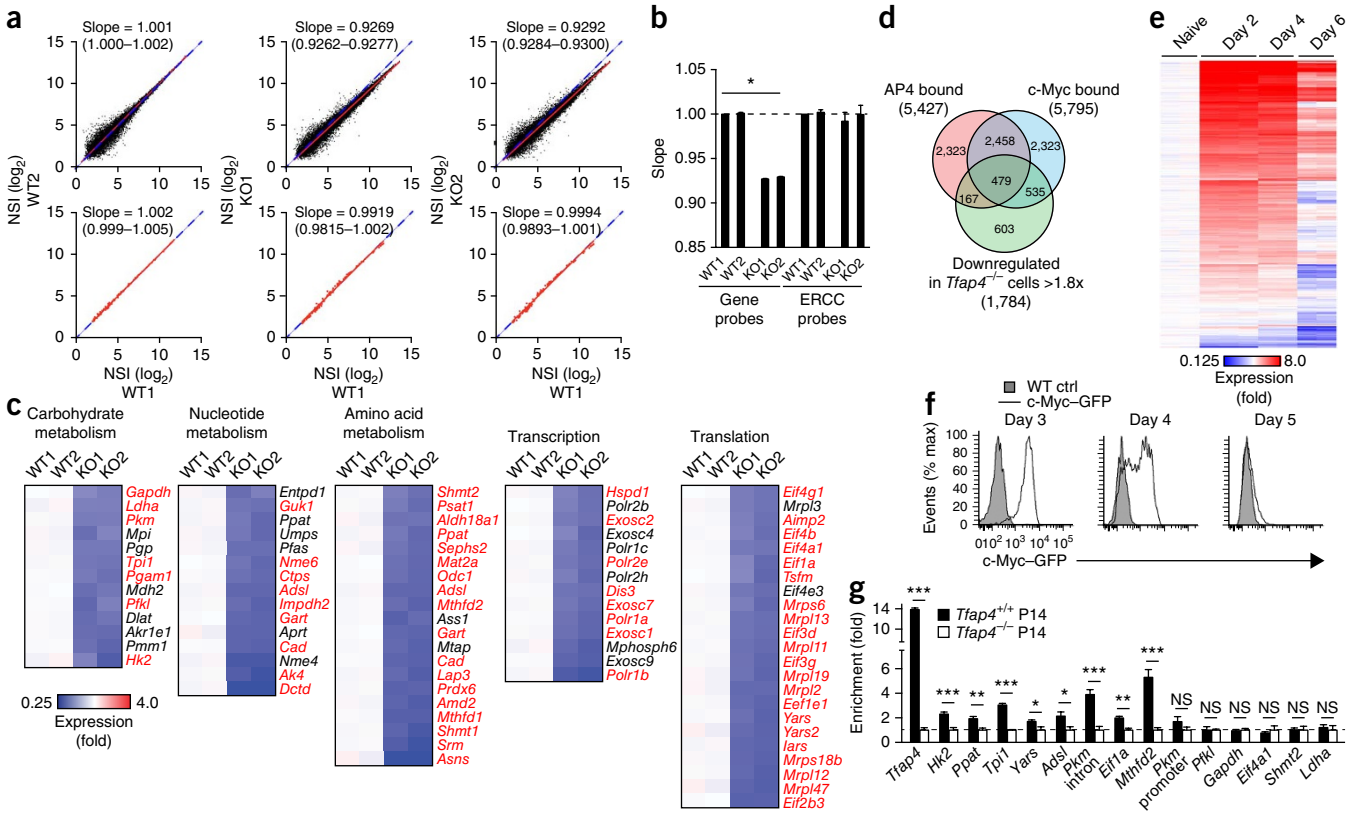

Figure 6 AP4 is essential for the sustained expression of genes that are targets of c-Myc. (**a**) Normalized signal intensity (NSI) of endogenous transcripts in *Tfap4*$^{+/+}$ and *Tfap4*$^{-/-}$ OT-I donor T cells adoptively transferred into host mice and assessed on day 4 after infection of the host with LM-OVA (top), and that of ERCC control RNA (bottom); numbers in plots indicate slope values obtained by linear regression (with 95% confidence interval in parentheses); slope of blue dashed lines, 1. WT1 and WT2, and KO1 and KO2, indicate two biological replicates of *Tfap4*$^{+/+}$ OT-I samples and of *Tfap4*$^{-/-}$ OT-I samples, respectively (throughout). (**b**) Slopes of plots in **a**. (**c**) Heat maps of the expression of genes encoding molecules in pathways (top) identified by the bioinformatics database DAVID (version 6.7), assessed in cells as in **a** and presented relative to results for *Tfap4*$^{+/+}$ OT-I T cells; red indicates genes bound by both c-Myc and AP4. (**d**) Overlap of AP4-bound genes, c-Myc-bound genes and genes expressed differently in *Tfap4*$^{-/-}$ cells relative to their expression in *Tfap4*$^{+/+}$ cells. (**e**) Kinetics of expression of the 479 genes identified in **d** (middle) in *Tfap4*$^{+/+}$ OT-I T cells adoptively transferred into host mice and assessed before (Naive) and on days 2, 4 and 6 after infection of the host with LM-OVA; results are presented relative to those of naive cells, set as 1. (**f**) Fluorescence of GFP in *Tfap4*$^{+/+}$ P14 T cells (WT ctrl) and P14 T cells carrying a knock-in allele encoding c-Myc–GFP (c-Myc–GFP), adoptively transferred together into host mice and assessed by fow cytometry on days 3–5 after infection of the host with LCMV-Arm. (**g**) ChIP and quantitative PCR analysis of the binding of AP4 to genes targeted by both AP4 and c-Myc in *Tfap4*$^{+/+}$ P14 T cells adoptively transferred into host mice and assessed on day 5 after infection with LCMV-Arm; results are presented as 'enrichment' relative to the binding in their *Tfap4*$^{-/-}$ counterparts, set as 1 (dashed line). *$P < 0.05$, **$P < 0.01$ and ***$P < 0.001$ (unpaired *t*-test). Data are from one experiment with two biological replicates (**a**–**e**; error bars (**b**), 95% confidence interval), are representative of two experiments (**f**) or are pooled from three experiments (**g**; error bars, s.d.).

AP4 supplements c-Myc function

Our data thus far suggested overlapping functions for AP4 and c-Myc in activated CD8$^+$ T cells. To determine whether AP4 was dispensable if c-Myc expression was sustained, we retrovirally expressed a stabilized form of c-Myc (with substitution of alanine for threonine at position 58 (c-Myc(T58A))[38,39]) in *Tfap4*$^{-/-}$ OT-I T cells in a culture system that recapitulated the difference between *Tfap4*$^{-/-}$ and wild-type cells in cell size. In this assay, we primed *Tfap4*$^{-/-}$ and *Tfap4*$^{+/+}$ OT-I T cells for 2 d *in vitro* with anti-CD3 and anti-CD28 and subsequently cultured the cells for 24 h with irradiated splenocytes pulsed with 1 pM OVA peptide. Ectopic expression of c-Myc(T58A) or AP4 itself in *Tfap4*$^{-/-}$ OT-I T cells 'rescued' the defects in cell size under these conditions (**Fig. 7a**,**b**). Overexpression of c-Myc(T58A) or AP4 also restored glycolysis, incorporation of BrdU and expression of a subset of genes regulated by both AP4 and c-Myc (**Fig. 7c**–**e**). To determine whether c-Myc(T58A) expression restored the clonal expansion of *Tfap4*$^{-/-}$ CD8$^+$ T cells *in vivo*, we transduced naive *Tfap4*$^{-/-}$ OT-I T cells with retrovirus to express c-Myc(T58A) or AP4 and transduced *Tfap4*$^{+/+}$ OT-I T cells with empty retrovirus, then adoptively transferred those cells into congenic wild-type host mice, followed by infection of the hosts with LM-OVA. Although retroviral expression of AP4 in *Tfap4*$^{-/-}$ OT-I T cells fully restored their clonal expansion and expression of the differentiation marker KLRG1, c-Myc(T58A) expression only partially restored clonal expansion (**Fig. 7f**–**h**). Nevertheless, c-Myc(T58A) expression increased the size and BrdU incorporation of *Tfap4*$^{-/-}$ OT-I cells similarly to AP4 ectopic expression (**Fig. 7i**,**j**). These results suggested that AP4 and c-Myc had partially overlapping functions in regulating T cell activation and that a temporal switch from c-Myc to AP4 was necessary for optimal population expansion of CD8$^+$ T cells.

To determine whether ectopic expression of AP4 correspondingly 'rescued' the defects of *Myc*-deficient cells, we retrovirally expressed AP4 in CD8$^+$ T cells in which c-Myc was inducibly deleted (cells expressing a *lox*P-flanked allele encoding c-Myc (*Myc*^{F}) and a gene encoding Cre recombinase and a tamoxifen-inducible variant of the estrogen receptor (Cre-ER^{T2}) expressed from the ubiquitously expressed *Rosa26* locus (*Rosa26*-Cre-ER^{T2}))[40,41]. To express AP4,

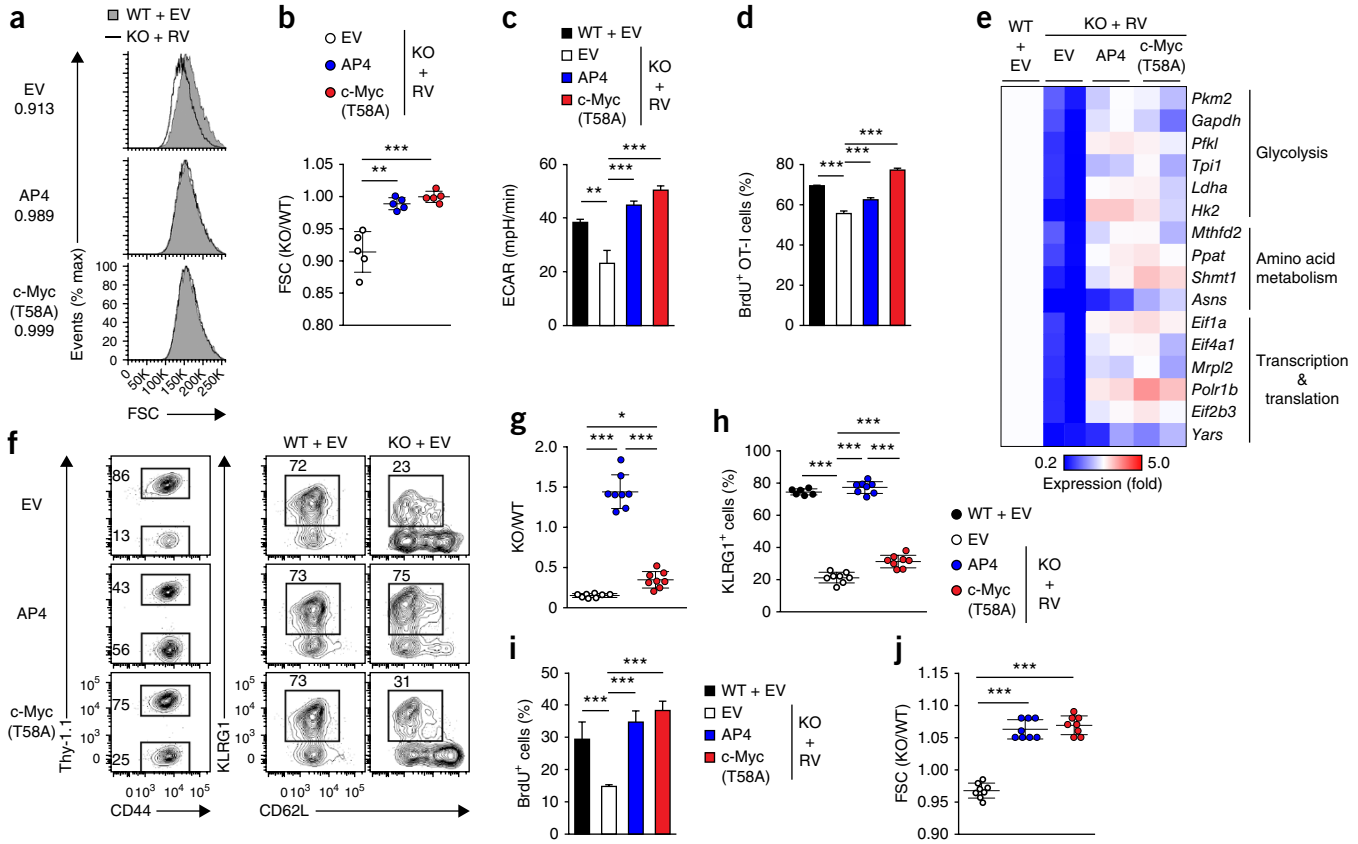

Figure 7 Sustained c-Myc expression 'rescues' defects of *Tfap4*$^{-/-}$ CD8$^+$ T cells. (**a**) Flow cytometry of *Tfap4*$^{+/+}$ OT-I (control) T cells transduced with retrovirus containing an empty vector (WT + EV) cultured with *Tfap4*$^{-/-}$ OT-I T cells (KO + RV) transduced with that retrovirus or retrovirus containing a vector for the expression of AP4 or c-Myc(T58A) (left margin). Numbers along left margin indicate ratio of the forward scatter of *Tfap4*$^{-/-}$ OT-I T cells to that of *Tfap4*$^{+/+}$ OT-I T cells. (**b**) Ratio of the forward scatter of *Tfap4*$^{-/-}$ OT-I T cells to that of *Tfap4*$^{+/+}$ OT-I T cells (all transduced as in **a**). (**c**,**d**) ECAR (**c**) and incorporation of BrdU (**d**) of *Tfap4*$^{+/+}$ and *Tfap4*$^{-/-}$ OT-I T cells transduced as in **a**. (**e**) Quantitative RT-PCR analysis of genes targeted by both AP4 and c-Myc (encoding molecules in various pathways (right margin)) in *Tfap4*$^{+/+}$ and *Tfap4*$^{-/-}$ OT-I T cells transduced as in **a**; results were normalized to those of 'spiked-in' RNA ERCC-108 and are presented relative to average results for the *Tfap4*$^{+/+}$ OT-I T cells. (**f**) Expression of Thy-1.1 and CD44 (left) and of KLRG1 and CD62L (right) in *Tfap4*$^{+/+}$ (Thy-1.1$^+$) and *Tfap4*$^{-/-}$ (Thy-1.1$^-$) OT-I T cells transduced as in **a** and adoptively transferred into congenic wild-type host mice, assessed by on day 6 after infection of the host with LM-OVA. Numbers adjacent to outlined areas indicate percent cells in each. (**g**–**j**) Ratio of *Tfap4*$^{-/-}$ OT-I T cells to *Tfap4*$^{+/+}$ OT-I T cells (KO/WT), all transduced as in **a** (**g**), and frequency of KLRG1$^+$ cells (**h**), incorporation of BrdU (**i**) and FSC ratio (as in **b**) (**j**) among *Tfap4*$^{+/+}$ and *Tfap4*$^{-/-}$ OT-I T cells transduced as in **a**. Each symbol (**b**,**g**,**h**,**j**) represents an individual mouse; small horizontal lines indicate the mean (± s.d.). $*P < 0.05$, $*P < 0.01$ and $***P < 0.001$ (one-way ANOVA). Data are representative of five (**a**), three (**c**) or two (**d**,**f**) experiments or are pooled from three (**b**) or two (**e**,**g**–**j**) experiments (error bars (**c**,**d**,**i**), s.d.).

we stimulated CD8$^+$ T cells from *Myc*$^{F/F}$*Rosa26*-Cre-ER^{T2} mice (called '*Myc*$^{-/-}$ mice' here) and control *Myc*$^{F/+}$Cre$^-$ or *Myc*$^{+/+}$*Rosa26*-Cre-ER^{T2} mice for 24 h *in vitro* with anti-CD3 and anti-CD28, then infected the cells with retrovirus, followed by treatment for 2 d with 4-hydroxytamoxifen under resting conditions. Subsequently, we assessed the proliferation and gene expression of transduced cells upon restimulation with anti-CD3 and anti-CD28 (**Supplementary Fig. 7a–c**). Retroviral c-Myc expression 'rescued', albeit partially, the proliferation and size increase of *Myc*$^{-/-}$ cells (**Supplementary Fig. 7d**), presumably because of a delay in expression of retrovirus-derived c-Myc compared with that of endogenous c-Myc upon restimulation (**Supplementary Fig. 7c**). In contrast, ectopic expression of AP4 failed to 'rescue' the defects of *Myc*$^{-/-}$ cells (**Supplementary Fig. 7d**). Accordingly, gene-expression profiling revealed little difference between *Myc*$^{-/-}$ cells transduced with retrovirus encoding AP4- and those transduced with empty retrovirus and that transduction with retrovirus encoding c-Myc partially 'rescued' gene expression (**Supplementary Fig. 7e**). These results indicated that AP4 required prior expression of c-Myc to mediate its effects. Thus, AP4 functionally supplemented c-Myc activity to prolong the activation of CD8$^+$ T cells.

DISCUSSION

Our study has defined a critical role for AP4 in regulating the clonal expansion and antiviral function of CD8$^+$ T cells. AP4 regulated the maintenance but not the initiation of rapid clonal expansion after priming. AP4 was dispensable for control of infection with LCMV-Arm or LM-OVA, as clearance of these microbes occurred rapidly and full clonal expansion of antigen-specific CD8$^+$ T cell was not necessary. In contrast, AP4 expression in CD8$^+$ T cells was essential for protection against neurotropic infection with WNV, because control of WNV in the CNS required the sustained activity of antigen-specific CD8$^+$ T cells. The increased susceptibility could have been due to reduced clonal expansion, leading to fewer cells' reaching the tissue (quantitative defects) or to defective differentiation as effector cells (qualitative defects). Our data suggest that AP4 is required predominantly for sustained rapid proliferation.

Mechanistically, there are two main possible interpretations for the function of AP4 in regulating acute responses of CD8$^+$ T cells. One

interpretation is direct regulation by AP4 of genes encoding molecules essential for T cell activation. The identification of AP4- and c-Myc-bound genes in CD8$^+$ T cells revealed a substantial overlap between targets of these two transcription factors. Combined analysis of ChIP data and gene-expression data showed that approximately a quarter of the genes expressed differently in *Tfap4*$^{-/-}$ cells were shared binding targets of AP4 and c-Myc. Among those 1,748 genes, we specifically examined a subset encoding molecules categorized as being involved in metabolism, general transcription or translation pathways and found approximately three quarters of that subset were binding targets shared by both AP4 and c-Myc, in support of the hypothesis that AP4 contributes to maintenance of T cell activation by regulating these genes. AP4 was dispensable for initial upregulation of these genes upon T cell priming, because these pathways are initially activated by c-Myc. In contrast, after downregulation of c-Myc expression during the late phase of the acute response, the contribution of AP4 to the regulation of these genes may become critical for the maintenance of expression. AP4 bound to these loci not only in CD8$^+$ T cells activated *in vitro* but also in those activated *in vivo* after c-Myc expression waned. In the context of cellular carbohydrate metabolism, the group of genes with different expression showed enrichment for those encoding enzymes but not transporters, which suggested the altered glucose use of *Tfap4*$^{-/-}$ CD8$^+$ T cells resulted from defective glycolysis rather than defective uptake of glucose. In contrast, since many genes encoding enzymes for glutaminolysis, amino acid transporters, and components of protein-translation machinery were downregulated in *Tfap4*$^{-/-}$ CD8$^+$ T cells, the smaller size of these cells probably reflected diminished protein synthesis resulting from defects at multiple stages. Since expression of *Hif1a* (which encodes the transcription factor HIF-1α) and components of the mTOR pathway was not reduced, the diminished activity of the mTOR pathway may have been regulated indirectly by AP4.

As an alternative explanation, AP4 might indirectly sustain the activity of T cells through sensitizing T cell activation independently of c-Myc. Sensitivity to extrinsic stimuli might not be important for the initial activation of CD8$^+$ T cells in the presence of abundant antigen or inflammatory cytokines. However, it may be critical in the late phase of the CD8$^+$ T cell response *in vivo* due to decreases in concentrations of antigens and cytokines. Under these circumstances, *Tfap4*$^{-/-}$ cells might prematurely lose activation, leading to their reduced metabolic activity and clonal expansion. A published study of *L. monocytogenes* expressing altered OVA peptide ligands has demonstrated that duration and magnitude of antigen-specific CD8$^+$ T cell responses *in vivo* are determined by affinity between the TCR and peptide ligands[42]. LM-OVA strains engineered to express variant epitopes of low affinity induced less clonal expansion of OT-I T cells at the peak than did LM-OVA expressing the canonical SIINFEKL epitope, despite normal initial activation[42]. Although the reduced clonal expansion induced by low-affinity peptide ligands is similar to the diminished population expansion of CD8$^+$ T cells in *Tfap4*$^{-/-}$ mice, there are differences. Infection with *L. monocytogenes* expressing low-affinity ligands shortens the duration of clonal expansion by triggering earlier contraction and also generates reduced numbers of memory cells after clearance of the infection[42]. We observed neither of those phenotypes in *Tfap4*$^{-/-}$ mice after infection with LM-OVA or LCMV-Arm.

Although we favor the former interpretation of AP4-dependent maintenance of c-Myc-regulated genes, the two models are not mutually exclusive. Regardless of that, our results indicate that c-Myc-induced expression of AP4 is essential for maximal clonal expansion and sustained T cell activity in a temporally regulated manner. In conclusion, our study has demonstrated that AP4 was critical for the regulation of CD8$^+$ T cell–mediated acute antipathogen responses by sustaining, in the 'post-Myc' phase, the expression of genes encoding molecules involved in metabolism. Activated T cells used AP4 to maintain their activated states under conditions of threshold signaling for the complete elimination of pathogens.

METHODS

Methods and any associated references are available in the online version of the paper.

Accession codes. GEO: microarray and ChIP-seq data, GSE58081.

Note: Any Supplementary Information and Source Data files are available in the online version of the paper.

ACKNOWLEDGMENTS

We thank M.J. Bevan (University of Washington, Seattle) for LM-OVA; I. Taniuchi (RIKEN, Yokohama) and D.R. Littman (New York University) for CD8-Cre mice; B.P. Sleckman (Washington University School of Medicine) for c-Myc–GFP knock-in mice; F.W. Alt (Harvard Medical School) and D.R. Green (St. Jude Children's Research Hospital) for *Myc*^{F} mice; T. Hansen (Washington University School of Medicine) for the H-2K^b–OVA single-chain tetramer; S. Hsiung, J. Govero and M.J. Sunshine for technical assistance; and E. Oltz, C.-S. Hsieh and D.R. Littman for discussions and critical reading of the manuscript. Supported by the Lucille P. Markey Pathway Program (C.C.), the Burroughs Wellcome Fund (B.T.E.), the McDonnell International Scholars Academy at Washington University (C.-C.L.), the US National Institutes of Health (P30 AR048335 to the Rheumatic Diseases Core Center; R01 AI097244 to T.E.; and U54 AI081680 to M.S.D.), the Edward Mallinckrodt Jr. Foundation (T.E.) and the Washington University Institute of Clinical and Translational Sciences of the National Center for Advancing Translational Sciences of the US National Institutes of Health (UL1 TR000448).

AUTHOR CONTRIBUTIONS

T.E. designed the study with help from M.Ce., P.M.A., M.Co., E.L.P. and M.S.D.; C.C., A.K.P., J.D.C., S.P.P., C.-C.L., B.T.E. and T.E. did experiments; C.C., E.L.P., M.S.D. and T.E. analyzed data; and T.E. wrote the manuscript with editorial comments from the other authors.

COMPETING FINANCIAL INTERESTS

The authors declare no competing financial interests.

1. Kaech, S.M. & Wherry, E.J. Heterogeneity and cell-fate decisions in effector and memory CD8$^+$ T cell differentiation during viral infection. *Immunity* **27**, 393–405 (2007).
2. Zhang, N. & Bevan, M.J. CD8$^+$ T cells: foot soldiers of the immune system. *Immunity* **35**, 161–168 (2011).
3. Chang, C.H. *et al.* Posttranscriptional control of T cell effector function by aerobic glycolysis. *Cell* **153**, 1239–1251 (2013).
4. Kaech, S.M. & Cui, W. Transcriptional control of effector and memory CD8$^+$ T cell differentiation. *Nat. Rev. Immunol.* **12**, 749–761 (2012).
5. MacIver, N.J., Michalek, R.D. & Rathmell, J.C. Metabolic regulation of T lymphocytes. *Annu. Rev. Immunol.* **31**, 259–283 (2013).
6. van der Windt, G.J. & Pearce, E.L. Metabolic switching and fuel choice during T-cell differentiation and memory development. *Immunol. Rev.* **249**, 27–42 (2012).
7. Wang, R. & Green, D.R. Metabolic reprogramming and metabolic dependency in T cells. *Immunol. Rev.* **249**, 14–26 (2012).
8. Kim, J. *et al.* A Myc network accounts for similarities between embryonic stem and cancer cell transcription programs. *Cell* **143**, 313–324 (2010).
9. Nie, Z. *et al.* c-Myc is a universal amplifier of expressed genes in lymphocytes and embryonic stem cells. *Cell* **151**, 68–79 (2012).
10. Lin, C.Y. *et al.* Transcriptional amplification in tumor cells with elevated c-Myc. *Cell* **151**, 56–67 (2012).
11. Rahl, P.B. *et al.* c-Myc regulates transcriptional pause release. *Cell* **141**, 432–445 (2010).
12. Sinclair, L.V. *et al.* Control of amino-acid transport by antigen receptors coordinates the metabolic reprogramming essential for T cell differentiation. *Nat. Immunol.* **14**, 500–508 (2013).

13. Wang, R. *et al.* The transcription factor Myc controls metabolic reprogramming upon T lymphocyte activation. *Immunity* **35**, 871–882 (2011).
14. Kaech, S.M. & Ahmed, R. Memory CD8+ T cell differentiation: initial antigen encounter triggers a developmental program in naive cells. *Nat. Immunol.* **2**, 415–422 (2001).
15. Prlic, M., Hernandez-Hoyos, G. & Bevan, M.J. Duration of the initial TCR stimulus controls the magnitude but not functionality of the CD8+ T cell response. *J. Exp. Med.* **203**, 2135–2143 (2006).
16. Blair, D.A. *et al.* Duration of antigen availability influences the expansion and memory differentiation of T cells. *J. Immunol.* **187**, 2310–2321 (2011).
17. Porter, B.B. & Harty, J.T. The onset of CD8+-T-cell contraction is influenced by the peak of *Listeria monocytogenes* infection and antigen display. *Infect. Immun.* **74**, 1528–1536 (2006).
18. Best, J.A. *et al.* Transcriptional insights into the CD8+ T cell response to infection and memory T cell formation. *Nat. Immunol.* **14**, 404–412 (2013).
19. Williams, M.A., Tyznik, A.J. & Bevan, M.J. Interleukin-2 signals during priming are required for secondary expansion of CD8+ memory T cells. *Nature* **441**, 890–893 (2006).
20. Obar, J.J. *et al.* CD4+ T cell regulation of CD25 expression controls development of short-lived effector CD8+ T cells in primary and secondary responses. *Proc. Natl. Acad. Sci. USA* **107**, 193–198 (2010).
21. D'Souza, W.N. & Lefrancois, L. IL-2 is not required for the initiation of CD8 T cell cycling but sustains expansion. *J. Immunol.* **171**, 5727–5735 (2003).
22. Kalia, V. *et al.* Prolonged interleukin-2Rα expression on virus-specific CD8+ T cells favors terminal-effector differentiation *in vivo*. *Immunity* **32**, 91–103 (2010).
23. Pipkin, M.E. *et al.* Interleukin-2 and inflammation induce distinct transcriptional programs that promote the differentiation of effector cytolytic T cells. *Immunity* **32**, 79–90 (2010).
24. Egawa, T. & Littman, D.R. Transcription factor AP4 modulates reversible and epigenetic silencing of the *Cd4* gene. *Proc. Natl. Acad. Sci. USA* **108**, 14873–14878 (2011).
25. Hu, Y.F., Luscher, B., Admon, A., Mermod, N. & Tjian, R. Transcription factor AP-4 contains multiple dimerization domains that regulate dimer specificity. *Genes Dev.* **4**, 1741–1752 (1990).
26. Mermod, N., Williams, T.J. & Tjian, R. Enhancer binding factors AP-4 and AP-1 act in concert to activate SV40 late transcription *in vitro*. *Nature* **332**, 557–561 (1988).
27. Pircher, H., Burki, K., Lang, R., Hengartner, H. & Zinkernagel, R.M. Tolerance induction in double specific T-cell receptor transgenic mice varies with antigen. *Nature* **342**, 559–561 (1989).
28. Maekawa, Y. *et al.* Notch2 integrates signaling by the transcription factors RBP-J and CREB1 to promote T cell cytotoxicity. *Nat. Immunol.* **9**, 1140–1147 (2008).
29. Yoon, H., Kim, T.S. & Braciale, T.J. The cell cycle time of CD8+ T cells responding *in vivo* is controlled by the type of antigenic stimulus. *PLoS ONE* **5**, e15423 (2010).
30. Petersen, L.R. & Fischer, M. Unpredictable and difficult to control–the adolescence of West Nile virus. *N. Engl. J. Med.* **367**, 1281–1284 (2012).
31. Suthar, M.S., Diamond, M.S. & Gale, M. Jr. West Nile virus infection and immunity. *Nat. Rev. Microbiol.* **11**, 115–128 (2013).
32. Shrestha, B. & Diamond, M.S. Role of CD8+ T cells in control of West Nile virus infection. *J. Virol.* **78**, 8312–8321 (2004).
33. Wang, R. & Green, D.R. Metabolic checkpoints in activated T cells. *Nat. Immunol.* **13**, 907–915 (2012).
34. Jung, P., Menssen, A., Mayr, D. & Hermeking, H. AP4 encodes a c-MYC-inducible repressor of p21. *Proc. Natl. Acad. Sci. USA* **105**, 15046–15051 (2008).
35. Huang, C.Y.B.A.L., Walker, L.M., Bassing, C.H. & Sleckman, B.P. Dynamic regulation of c-Myc proto-oncogene expression during lymphocyte development revealed by a GFP-c-Myc knock-in mouse. *Eur. J. Immunol.* **38**, 342–349 (2008).
36. van der Windt, G.J. *et al.* Mitochondrial respiratory capacity is a critical regulator of CD8+ T cell memory development. *Immunity* **36**, 68–78 (2012).
37. Lovén, J. *et al.* Revisiting global gene expression analysis. *Cell* **151**, 476–482 (2012).
38. Chang, D.W., Claassen, G.F., Hann, S.R. & Cole, M.D. The c-Myc transactivation domain is a direct modulator of apoptotic versus proliferative signals. *Mol. Cell. Biol.* **20**, 4309–4319 (2000).
39. Yeh, E. *et al.* A signalling pathway controlling c-Myc degradation that impacts oncogenic transformation of human cells. *Nat. Cell Biol.* **6**, 308–318 (2004).
40. de Alboran, I.M. *et al.* Analysis of C-MYC function in normal cells via conditional gene-targeted mutation. *Immunity* **14**, 45–55 (2001).
41. Ventura, A. *et al.* Restoration of p53 function leads to tumour regression *in vivo*. *Nature* **445**, 661–665 (2007).
42. Zehn, D., Lee, S.Y. & Bevan, M.J. Complete but curtailed T-cell response to very low-affinity antigen. *Nature* **458**, 211–214 (2009).

ONLINE METHODS

Mice. Mice with a *lox*P-flanked *Tfap4* allele were generated essentially as described[24] in E14TG2a embryonic stem cells derived from the 129P2/Ola strain (**Supplementary Fig. 1a**). *Tfap4*$^{-/-}$ mice have been described[24]. Both AP4-mutant strains were backcrossed to C57BL/6 mice for more than ten generations before being intercrossed or bred with other transgenic mice. *Myc*^{F} mice and mice with the knock-in allele encoding c-Myc–GFP have been described[35,40]. C57BL/6 and B6-Ly5.2 (CD45.1^{+}) mice were from the National Cancer Institute. OT-I mice[43], *Tcra*$^{-/-}$ mice[44], *Il2ra*$^{-/-}$ mice[45], *Rosa26*-Cre-ER^{T2} mice[41] and C57BL/6 Thy-1.1^{+} mice were from the Jackson Laboratory, and P14 mice[28] were from Taconic. *Il2ra*$^{-/-}$ P14 T cells were collected from chimeric mice reconstituted with a mixture of bone marrow cells from *Il2ra*$^{-/-}$ (Thy-1.2^{+}) P14 mice and wild-type (Thy-1.1^{+}) P14 mice. CD8-Cre mice were generated previously on the C57BL/6 background[27]. All mice were maintained in a specific pathogen–free facility at Washington University in St. Louis, and all experiments were performed according to a protocol approved by Washington University's Animal Studies Committee. All mice were analyzed at 6–14 weeks of age, and both sexes were included without randomization or blinding.

Infection experiments. LCMV-Arm stocks were prepared by infection of BHK (baby hamster kidney) cells, followed by titering of culture supernatants by plaque assay on Vero (African green monkey kidney) cells. Mice were infected with 2×10^5 plaque-forming units of LCMV-Arm by intraperitoneal injection. Mice were given intravenous inoculation of LM-OVA at a dose of 1×10^4 colony-forming units. Infection with WNV (New York 1999 strain) was performed as described[32]. For adoptive transfer experiments, CD44^{-}CD62L^{+}V$_{\alpha}$2^{+}V$_{\beta}$5^{+} OT-I donor T cells or CD44^{-}CD62L^{+}V$_{\alpha}$2^{+}V$_{\beta}$8^{+} P14 donor T cells were purified by fluorescence-activated cell sorting, and 5×10^5 cells (for analysis at day 3), 1×10^4 to 2×10^4 (for analysis at day 4) or 1×10^4 to 3×10^4 cells (for analysis at days 5–12) were transferred intravenously into host mice 1 d before infection. All experiments using infectious agents were performed in biosafety level 2 and 3 facilities according to the protocols approved by Washington University Institutional Biological and Chemical Safety Committee.

Flow cytometry. Single-cell suspensions were prepared by manual disruption of spleens with frosted glass slides, followed by lysis of erythrocytes with ammonium chloride–potassium (ACK) solution, or by digestion of mesenteric lymph nodes, liver, lungs and kidneys with collagenase B and D (Roche), followed by purification with a Percoll gradient (GE Healthcare Life Sciences). The following monoclonal antibodies were used in this study: fluorescein isothiocyanate–conjugated anti-CD62L (MEL-14; Biolegend), anti-V$_{\alpha}$2 (B20.1; Biolegend) and anti-Thy-1.2 (53-2.1; eBioscience); phycoerythrin-conjugated anti-V$_{\beta}$5 (MR9-4; Biolegend), anti-V$_{\beta}$8 (KJ16-133.18; Biolegend), anti-CD25 (PC61; Biolegend), anti-KLRG1 (2F1/KLRG1; Biolegend) and anti-IFN-γ (XMG1.2; eBioscience); peridinin chlorophyll protein–cyanin 5.5–conjugated anti-CD4 (GK1.5; Biolegend), anti-Thy-1.1 (OX-7; Biolegend) and anti-V$_{\alpha}$2 (B20.1; Biolegend); phycoerythrin-indotricarbocyanine-conjugated anti-CD8α (53-6.7; Biolegend); allophycocyanin-conjugated anti-KLRG1 (2F1/KLRG1; Biolegend), anti-CD62L (MEL-14; eBioscience), anti-CD25 (PC61; eBioscience), anti-TCRβ (H57-597; eBioscience) and anti-CD45.2 (104; Biolegend); Alexa Fluor 700–conjugated anti-CD44 (IM7; Biolegend); allophycocyanin–indotricarbocyanine conjugated anti-CD45.2 (104; Biolegend); Pacific Blue–conjugated anti-CD44 (IM7; Biolegend); Brilliant Violet 421–conjugated anti-CD127 (A7R34; Biolegend); Brilliant Violet 510–conjugated anti-B220 (RA3-6B2; Biolegend); and Brilliant Violet 605–conjugated anti-CD45.1 (A20; Biolegend). For sorting of naive CD8^{+} T cells, splenocyte samples were initially depleted of B220^{+} cells through the use of magnetic beads (Life Technologies) and then were stained with monoclonal antibodies (identified above) before being sorted as CD62L^{+}CD44^{-}CD8^{+}CD4^{-} cells on a FACSAria II (BD Biosciences). For analysis, cells were stained with monoclonal antibodies (identified above), phycoerythrin-conjugated H-2D^{b}–gp(33–41) (Beckman Coulter) or H2-K^{b}–OVA single-chain tetramer and were analyzed with an LSR II (BD Biosciences),with staining with DAPI (4,6-diamidino-2-phenylindole; Sigma) for the exclusion of dead cells. Data were analyzed with FlowJo software (TreeStar). For intracellular staining of AP4, cells were fixed for 10 min with 2% paraformaldehyde (PFA; Electron Microscopy Sciences) and permeabilized for 30 min with ice-cold 100% methanol and then markers were stained with fluorochrome-conjugated monoclonal antibodies (identified above), and AP4 was stained with affinity-purified polyclonal antibody to AP4 (ref. 24), at a concentration of 1.25 μg/ml, followed by Alexa Fluor 647–conjugated secondary antibody to rabbit IgG (4414S; Cell Signaling). For detection of phosphorylated ribosomal protein S6, cells were fixed with PFA and permeabilized with methanol, and surface markers were stained and phosphorylation of S6 was detected with antibody to phosphorylated S6 (4858; Cell Signaling) and Alexa Fluor 647–conjugated secondary antibody to rabbit IgG (Cell Signaling).

BrdU labeling. At various time points after infection, mice were given intraperitoneal injection of 1 mg BrdU (5-bromodeoxyuridine) 2 h before being killed. The incorporation of BrdU was analyzed with an APC-BrdU Flow Kit according to the manufacturer's instructions (552598; BD Biosciences). For proliferation assays *in vitro*, cells were cultured in medium containing 10 μM BrdU for 1 h before analysis.

***In vitro* stimulation of T cells.** Naive CD8^{+} T cells were cultured in RPMI medium supplemented with 10% FBS (Life Technologies) in the presence of soluble anti-CD3 (145-2C11; Biolegend) and anti-CD28 (37.51; Bio X Cell) at concentrations of 0.1 μg/ml and 1 μg/ml, respectively, unless specified otherwise, in multiwell tissue culture plates coated with rabbit antibody to hamster IgG (0855395; MP Biomedicals). For retroviral transduction of activated T cells, viral supernatants were prepared by transfection of PlatE packaging cells[46] with TransIT 293 (Mirus Bio), and primed T cells were 'spin-inoculated' following overnight stimulation as described[24]. For retroviral transduction of CD8^{+} T cells without stimulation of the TCR, naive CD8^{+} T cells were cultured for 2 d in the presence of IL-7 (10 ng/ml; Peprotech) and IL-15 (100 ng/ml, Peprotech) before 'spin-inoculation'. For blockade of IL-2, 2 μg/ml of anti-IL-2 (JES6-1A12; Biolegend) was added to the culture.

Real-time quantitative RT-PCR. RNA was extracted with Trizol (Life Technologies) and was reverse-transcribed with qScript Supermix (Quanta Bio). DyNAmo ColorFlash SYBR green qPCR mix (Thermofisher) and a LightCycler 480 (Roche) were used for real-time quantitative RT-PCR. Quantities of transcripts were normalized to that of 18S ribosomal RNA unless specified otherwise. For quantification of gene expression normalized to that of 'spiked-in' RNA, 1 μl of ERCC (External RNA Controls Consortium) RNA Spike-In Control Mixes (Ambion) was added, at a of dilution of 1:1,000, to total RNA extracted from 1×10^5 cells before reverse transcription. The mixed RNA was used for reverse transcription and real-time PCR quanfication. The following primers were used: 18S-rRNA, CGGCTACCACATCCAAGGAA and GCTGGAATTACCGCGGCT; *Bcl6*, CCTGTGAAATCTGTGGCACTCG and CGCAGTTGGCTTTTGTGACG; *Eomes*, ACCCAGCTAAAGATCGACCA and GACCTCCAGGGACAATCTGA; *Gapdh*, CTCACAATTTCCATCCCAGACC and CATCAATGGTGCAGC GAACTTTATTGATG; *Hif1a*, CTGGAAACGAGTGAAAGGATTC and CGTAACTGGTCAGCTGTGGTAA; *Hk2*, CAACTCCGGATGGGACAG and CACACGGAAGTTGGTTCCTC; *Hprt1*, AGGTTGCAAGCTTGCTGGT and TG AAGTACTCATTATAGTCAAGGGCA; *Il2ra*, CTCACCTGGCAACACAGATG and GGCTCTGACTTTTCTAGCTTGC; *Ldha*, CTGTTGGCATGGCTTGTG and CATCATCTCGCCCTTGAGTT; *Myc*: AGTGCTGCATGAGGAGACAC and GGTTTGCCTCTTCTCCACAG; *Pkm2*, CTGTCTGGAGAAAC AGCCAAG and TCGAATAGCTGCAAGTGGTAGA; *Slc2a1*, ATGG ATCCCAGCAGCAAG and CCAGTGTTATAGCCGAACTGC; *Tfap4*, GG AGAAGCTAGAGCGGGAAC and TTTTGCCGGGATGTAGAGAC; ERCC00108, CTATCAGCTTGCGCCTATTAT and GTTGAGTCCACG GGATAGAGTC; and LCMV-GP, CATTCACCTGGACTTTGTCAGACTC and GCAACTGCTGTGTTCCCGAAAC.

Microarray analysis. Total RNA was extracted with a Nucleospin RNA XS extraction kit (Macherey-Nagel). 5–50 ng of total RNA was amplified with a PicoSL RNA amplification kit (Nugen), followed by biotinylation with an Encore biotin module (Nugen). Labeled RNA was hybridized to a Mouse Gene 1.0ST microarray according to the manufacturer's instruction (Affymetrix). Data were analyzed with Arraystar software (DNA Star) with normalization by

doi:10.1038/ni.2943

the robust multi-array average method[47]. For microarray analysis of 'spiked-in' RNA, ERCC RNA Spike-In Control Mixes were added as described above, followed by amplification, labeling and hybridization of RNA. CEL files were generated with a modified CDF file provided by Affymetrix. Data were initially normalized by the robust multi-array average method, and signal intensities were further converted by a formula obtained from linear regression of normalized signal intensities of probes for spiked-in control RNA in one *Tfap4*$^{+/+}$ sample versus the other *Tfap4*$^{+/+}$ or *Tfap4*$^{-/-}$ samples.

ChIP. CD8$^+$ T cells were purified from C57BL/6 mice by positive selection with FlowComp CD8 Dynabeads (Life Technologies). Purified CD8$^+$ T cells were stimulated for 2 d with anti-CD3 and anti-CD28 (identified above), and were fixed for 10 min at room temperature with 1% PFA. Chromatin was sheared and immunoprecipitated as described[48]. Anti-AP4 has been described[24]. Anti-c-Myc (sc-764) and antibody to phosphorylated RNA polymerase II (ab5095 and ab5131) were from Santa Cruz and Abcam, respectively. After immunoprecipitation, DNA was purified with a purification kit (Sigma), and 1–10 ng of DNA was used for library construction, followed by 50–base pair single-read sequencing on a HiSeq2000 system (Illumina). Sequence tags were mapped onto the NCBI37 mm9 National Center for Biotechnology Information assembly of mouse genome with Bowtie2 software for the alignment of short DNA sequences[49] with the default setting. BedGraph histograms normalized to 1×10^7 'reads' were generated with the Homer suite of tools for motif discovery and next-generation sequencing analysis ('hypergeometric optimization of motif enrichment')[50] and were visualized with the IGV tool for the visualization of genomic data sets ('integrative genomics viewer'). Homer was used for peak 'calling' with a –style factor option and Poisson *P* value cutoff of 1×10^{-65} for AP4 and 5×10^{-9} for c-Myc for extraction of the 7,000 peaks with the highest statistical significance. For analysis of overlapping binding targets and binding motifs, 7,000 AP4-binding peaks filtered by a *P* value of $< 1.5 \times 10^{-65}$ and 7,000 c-Myc-binding peaks ($P < 5 \times 10^{-9}$) were analyzed. The following primers were used for real-time PCR analysis: *Adsl*, GGAATAATTCTGACAGGC TGCT and GCCCTAGTGGACACTTGGAGTA; *Cd4* (promoter), TGGCCTTGAGCTTGTGATTTTTCT and GAATCAAGCTGG AGTCTGGAATGT; *Cd4* (silencer), TACGAAGCTAGGCAACAGAGGAAG and TGTGGTCCCGAATGCGTTT; *Eif1a*, ATCACCAAACAGGCAAGA TTTC and GGGTTGCCCTTTTTACATTTCT; *Eif4a1*, ACAACA GACAAGCGAAACAGG and ACATGGCCGCTTGAGAGATT; *Gapdh*, CGCGAGGCTAGAACTTCTCC and TAGTAATCCAACACCCCGACTT; *Hk2*, AGGCCTCTTCAACACATCCTTA and GTGGGGAAGAATCCTGCTTAG; *Hoxa13*, TTGTTTCCTGTTGGTTCCAG and AGCCCAAACTTCCCAGAGA; *Ldha*, CTTCTGAGGCTGAGGAGCAT and CACGATGTCCCTGCAAGAGT; *Mthfd2*, TGAGGCATTGCAGATTACCATA and CTGTCATACGAGCAG ACACAGG; *Pfkl*, GGCTGTGCTTCTCTTAGAGGTC and CTATTCCTTT CTAGGCCACACG; *Pkm* (promoter), AGCGACTCGTCTTCACTTGACT and GTTCCTGCTGCGATACCTAGAG; *Pkm* (intron), CTACTCAGGTT TGGAGGTGGTC and GAGATGCTCAGAGCTCCCTAGA; *Ppat*, CACCCAAACACACCACATTC and CCTCTTGAGGCGTTCGATAG; *Shmt2*, AGCAAAGAGAAGGATACCATCG and GCCTCTTTCACTCGAACTTCAC; *Tfap4* (promoter), CTGATCAGATGTCTGTTTCAAGG and CGCTGCAAATA GTCCTTTGTTT; *Tfap4* CNS1 (Myc-1), CGAGTAAGCAAGGAAAAGGAAG and AGTCGCGACGTTTGTAAATTG; *Tfap4* CNS2 (Myc-2), GACCCGGCAT AGAGAACTACAG and AGTCACTAGTCGCACGTTCTCC; *Tpi1*, GATGTCA AGGAAGGGGGTCT and GTGCAGACCTCTCGAATAGCC; and *Yars*, ATCGATTCTTTCGACTCTCTGC and GGGAACTGTCACGCTAGTCC.

Metabolic measurements. ECAR was measured with a Seahorse XF96 Analyzer (Seahorse Bioscience) essentially as described[36]. CD8$^+$ T cells were purified from uninfected mice (for naive) or chimeric mice given transfer of a mixture of *Tfap4*$^{+/+}$ OT-I and *Tfap4*$^{-/-}$ OT-I T cells and infected with 1×10^4 colony-forming units of LM-OVA. For the preparation of *in vitro*–activated CD8$^+$ T cells, purified naive CD8$^+$ T cells were activated for 24 h with anti-CD3 and anti-CD28 (identified above) without exogenous IL-2. CD8$^+$ T cells (0.15×10^6 per well) from were seeded onto a 96-well plate and ECAR was measured in XF medium (unbuffered RPMI-1640 medium containing 25 mM glucose, 2 mM L-glutamine and 1 mM sodium pyruvate) under basal conditions and in response to 1 μM oligomycin.

Immunoblot analysis. Whole cell extracts were prepared by lysis of cells in Laemmli buffer containing 1% SDS and 2% 2-mercaptoethanol. Lysates from equal numbers of cells were separated by 8% or 10% SDS PAGE and transferred to PVDF membranes (GE Healthcare), which were incubated with primary antibodies (identified below), followed by detection with horseradish peroxidase–conjugated species-specific antibody to immunoglobulin light chain (115-035-174 or 211-032-171; Jackson ImmunoResearch) and a Luminata HRP substrate (Millipore). Anti-HDAC1 (ab7028; Abcam) and anti-β-tubulin (Developmental Studies Hybridoma Bank, University of Iowa) were used as loading controls. Anti-AP4 has been described[24]. The following antibodies were also used: anti-c-Myc (9402S; Cell Signaling), antibody to STAT5 phosphorylated at Tyr694 (611964; BD Biosciences), anti-Blimp-1 (A01647-40; Genscript), anti-T-bet (sc-21003; Santa Cruz). For inhibition of translation and proteasomes, 10 μM cycloheximide (Sigma) or MG132 (Sigma) was added to the cell culture. For inhibition of signaling pathways, 20 nM U0126 (Cayman Chemical), 10 μM SB203580 (Cayman Chemical), 50 nM wortmannin (Cayman Chemical), 5 nM FK506 (Cayman Chemical) or 2.5 nM rapamycin (Cayman Chemical) was added to the cell culture.

Statistical analysis. *P* values were calculated with an unpaired two-tailed Student's *t*-test for two-group comparisons and by one-way ANOVA for multiple-group comparisons with the Tukey post-hoc test in Prism 6 software (Graphpad) unless specified otherwise. *P* values of <0.05 were considered significant.

43. Hogquist, K.A. *et al.* T cell receptor antagonist peptides induce positive selection. *Cell* **76**, 17–27 (1994).
44. Mombaerts, P. *et al.* Mutations in T-cell antigen receptor genes α and β block thymocyte development at different stages. *Nature* **360**, 225–231 (1992).
45. Willerford, D.M. *et al.* Interleukin-2 receptor α chain regulates the size and content of the peripheral lymphoid compartment. *Immunity* **3**, 521–530 (1995).
46. Morita, S., Kojima, T. & Kitamura, T. Plat-E: an efficient and stable system for transient packaging of retroviruses. *Gene Ther.* **7**, 1063–1066 (2000).
47. Bolstad, B.M., Irizarry, R.A., Astrand, M. & Speed, T.P. A comparison of normalization methods for high density oligonucleotide array data based on variance and bias. *Bioinformatics* **19**, 185–193 (2003).
48. Ciofani, M. *et al.* A validated regulatory network for Th17 cell specification. *Cell* **151**, 289–303 (2012).
49. Langmead, B. & Salzberg, S.L. Fast gapped-read alignment with Bowtie 2. *Nat. Methods* **9**, 357–359 (2012).
50. Heinz, S. *et al.* Simple combinations of lineage-determining transcription factors prime cis-regulatory elements required for macrophage and B cell identities. *Mol. Cell* **38**, 576–589 (2010).